SUPPLEMENTAL MATERIAL

McCloskey et al., http://www.jem.org/cgi/content/full/jem.20100354/DC1

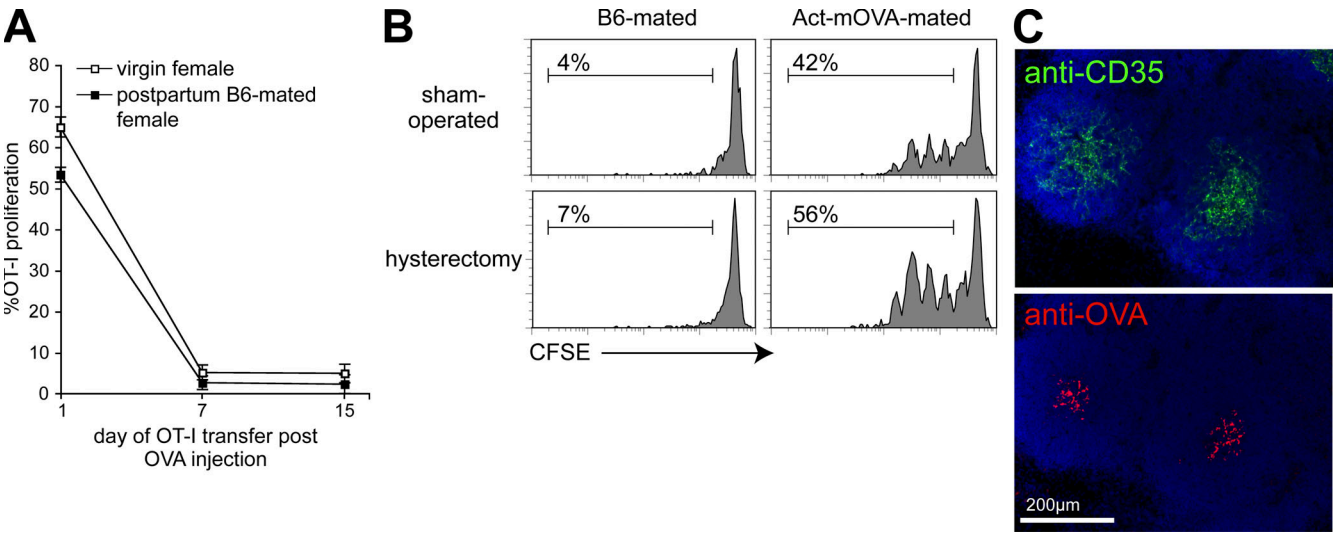

Figure S1. Normal DC life-spans in the postpartum period and uterine independence of persistent antigen presentation. (A) Kinetics of soluble OVA presentation in postpartum females. Virgin or B6-mated postpartum females (within 5 d of delivery) were injected intravenously with 100 µg OVA and then given CFSE-labeled OT-I cells 1, 7, or 15 d later. T cell proliferation in subcutaneous LNs was assessed 44 h after OT-I transfer. The percentage of OT-I cells having undergone more than one division cycle is shown, after subtracting out the baseline level of cell division (~1–4%) apparent in virgin controls that had not received OVA. Results show mean ± SEM for $n = 3$ mice per group. Data are representative of two independent experiments. (B and C) Lack of effect of hysterectomies performed within 1 wk after delivery on postpartum placental OVA presentation and OVA retention by FDCs. (B) Mice received CFSE-labeled OT-I T cells 3 wk after hysterectomy or sham surgery, and cell proliferation was visualized by flow cytometry 44 h later. The experiment was performed three independent times; data show representative CFSE dilution plots. Robust proliferation was seen in 4 out of $n = 5$ mice for the Act-mOVA–mated, hysterectomized group and in 3 out of $n = 3$ mice for the Act-mOVA–mated, sham-operated group. The other two control groups contained $n = 3$ mice per group. (C) Immunohistochemistry of LN FDC networks in Act-mOVA–mated females 3 wk after hysterectomy. Serial LN tissue sections were stained with anti-CD35 and anti-OVA antibodies and counterstained with DAPI. Data are representative of $n = 4$ mice.

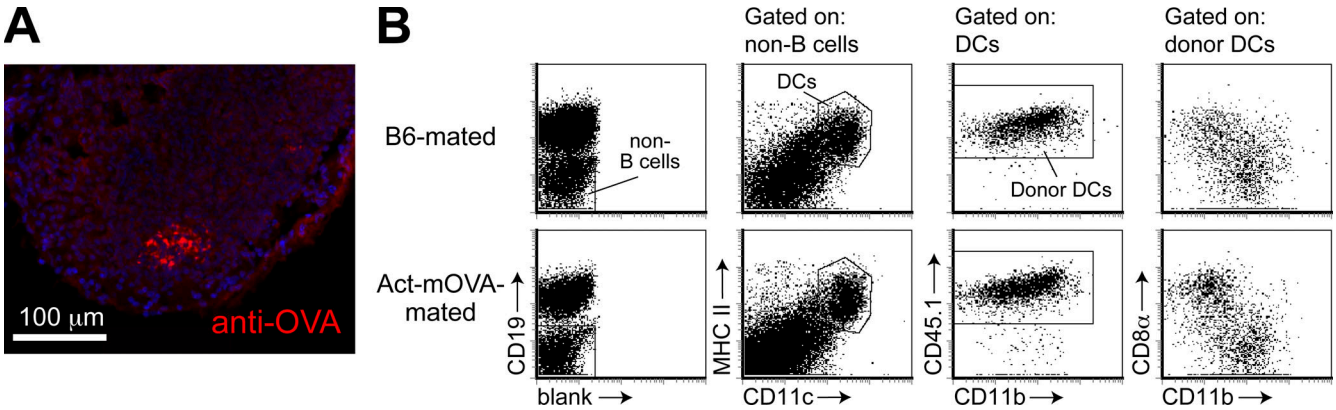

Figure S2. FDC-OVA retention and DC chimerism after bone marrow transfer. (A) Postpartum Act-mOVA–mated B6CBAF1 mice within 1 wk after delivery were transplanted with B6CBAF1 bone marrow cells using the γ-radiation/cyclophosphamide/NK bone marrow–conditioning regimen used in Fig. 2. 1 wk after the transplant, LN tissue sections were stained with antibodies to OVA and counterstained with DAPI (blue). Data are representative of $n = 2$ mice from one experiment. (B) DC chimerism in postpartum $K^{b-}D^{b-}$ B6CBAF1 mice transplanted with B6CBAF1 bone marrow. The gating strategy identifies splenic DCs as being $CD19^-$ $MHCII^+$ $CD11c^+$ and those of donor origin additionally being $CD45.1^+$. These cells divided into myeloid ($CD11b^+$ $CD8\alpha^-$) and lymphoid ($CD11b^-$ $CD8\alpha^+$) DC subsets. Data are representative of the $n = 5$–6 mice per group and three independent experiments shown in Fig. 2 B.

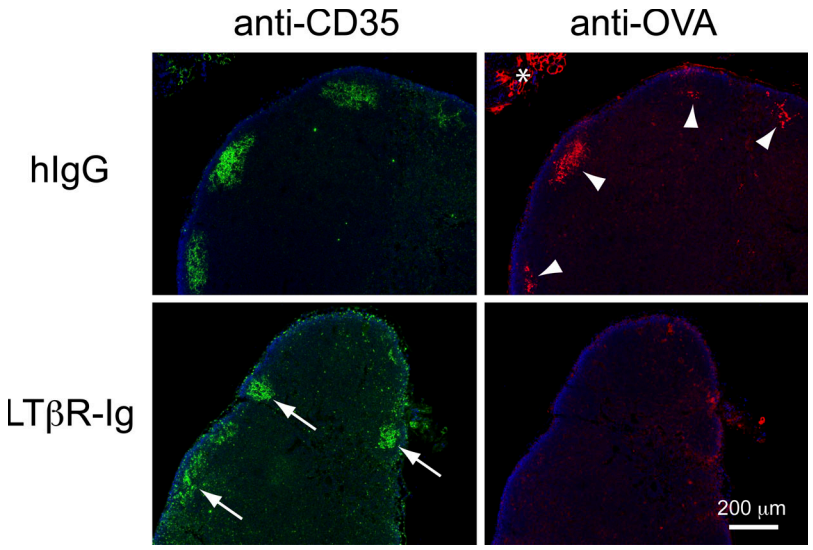

Figure S3. FDC status 3 wk after LTβR-Ig injection. Act-mOVA–mated B6CBAF1 females were injected with 100 µg LTβR-Ig or control hIgG within 1 wk after delivery and were sacrificed 3 wk later. LN tissue sections were stained with antibodies to CD35 (green) or OVA (red), which revealed the recovery of FDC networks in LTβR-Ig–treated mice (arrows) but their loss of FDC-associated OVA. OVA$^+$ FDC networks were still apparent in hIgG-treated controls (arrowheads). The asterisk indicates a nonspecific artifact seen in the absence of primary antibody. Data are representative of $n = 3$ mice per group from two independent experiments.

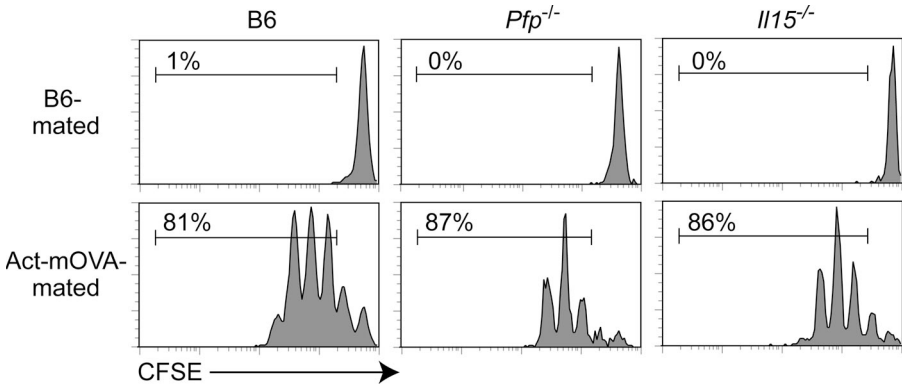

Figure S4. Systemic OT-I proliferation in Act-mOVA–mated mice is independent of perforin or IL-15. *Pfp*$^{-/-}$ and *Il15*$^{-/-}$ females or B6 controls were mated to B6 or Act-mOVA males, and antigen presentation was assessed in the spleen by injecting the mice with CFSE-labeled OT-I T cells on E14.5–19.5. Cell proliferation was then visualized 42–44 h later by flow cytometry. Data are representative of $n = 3$ Act-mOVA–mated mice per group from two independent experiments.

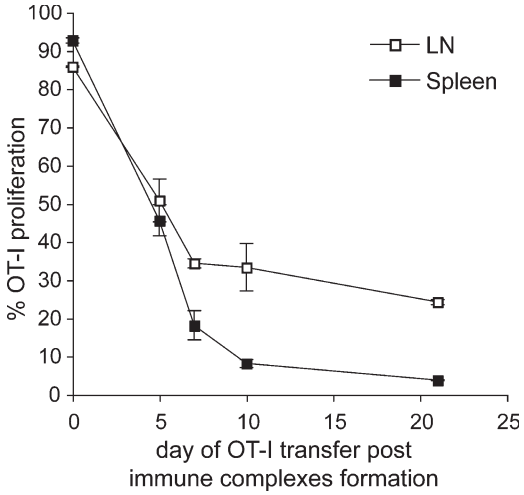

Figure S5. Presentation of OVA–anti-OVA immune complexes persists in the subcutaneous LNs but not the spleen. Mice were transferred with OT-I T cells on the indicated day after the injection of 100 µg soluble OVA and 250 µg rabbit anti-OVA antibodies to induce immune complex formation. The mice were sacrificed 44 h after OT-I transfer, and cell proliferation was visualized by flow cytometry. The percentage of OT-I cells having undergone more than one division cycle is shown. Results show mean ± SEM for $n = 2–5$ mice per group compiled from two independent experiments. Untreated mice showed 1–4% proliferation (not depicted).

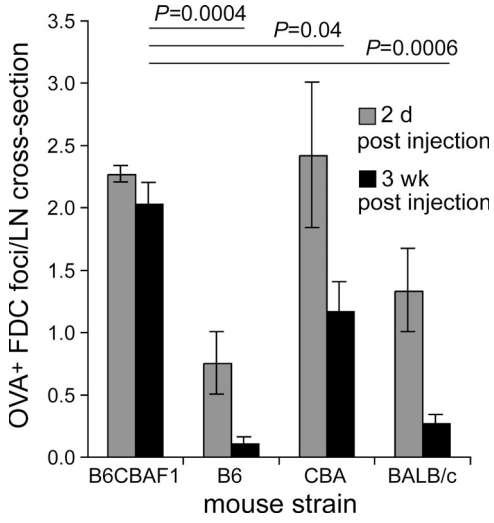

Figure S6. Different mouse strains show differential loading and long-term retention of immune complexes on LN FDCs. Virgin B6CBAF1, B6, CBA, and BALB/c females were injected intravenously with 250 µg rabbit anti-OVA followed by 100 µg OVA. Subcutaneous LNs were collected 2 d or 3 wk later, and tissue sections were stained with anti-OVA and anti-CD35 antibodies. The number of OVA^+ FDC networks per LN cross section is displayed ± SEM ($n = 2–3$ animals per group from one experiment).

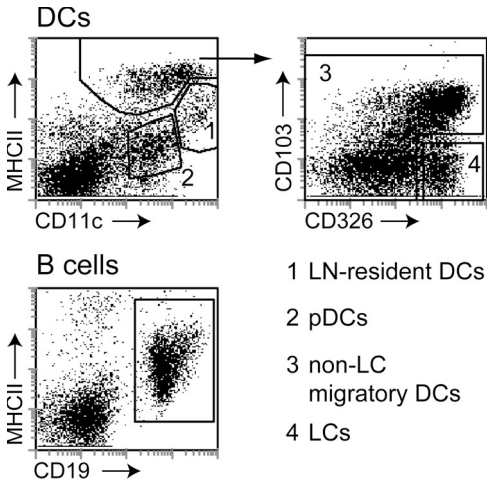

Figure S7. Sorting scheme for LN APCs. DC populations were identified in B cell–depleted subcutaneous LN cell suspensions with antibodies to MHCII, CD11c, CD103, and CD326; B cells were identified in B cell–enriched suspensions with antibodies to MHCII and CD19. LN-resident DCs were identified as CD11c^{hi} MHCII^{+} (gate 1); plasmacytoid DCs (pDCs) were CD11c^{int} MHCII$^{int\text{-}lo}$ (gate 2). Migratory (CD11c^{int} MHCII^{hi}) DCs were divided into CD103^{-} CD326^{hi} Langerhans cells (LCs; gate 4) and non–Langerhans cells (gate 4).

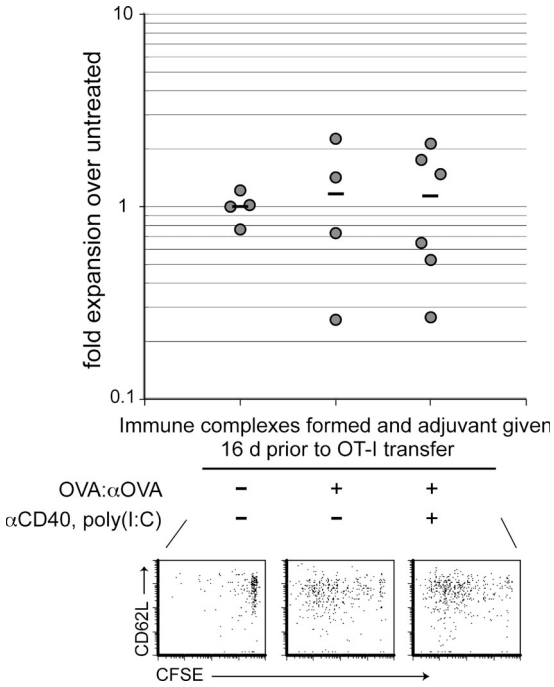

Figure S8. Immune complexes formed in the presence of adjuvants are tolerogenic when presented to CD8 T cells 3 wk later. Virgin B6CBAF1 mice were either left untreated or intravenously injected with 250 µg rabbit anti-OVA followed by 100 µg OVA to induce OVA–α-OVA immune complex formation. Some of these latter mice were also concomitantly injected with 30 µg α-CD40 plus 15 µg poly(I:C). The animals were then given CD45.1-marked, CFSE-labeled OT-I cells 16 d later, and cell proliferation and accumulation were assessed in the subcutaneous LNs 5 d later by flow cytometry. For each experiment, the fold OT-I expansion for each mouse was calculated by normalizing the OT-I/total CD8^{+} T cell ratio to the mean for this ratio in the virgin, untreated group. Individual mice are plotted as well as the mean fold expansion for each group (bars). Data are from n = 4–6 mice per group compiled over two independent experiments.